Conditional statistics for a passive scalar with a mean gradient and intermittency

A. Bourlioux, A. J. Majda, and O. Volkov
Département de Mathematics and Statistics, Université de Montréal, Montréal, Quebec H3C 3J7 Canada;
Courant Institute of Mathematical Sciences, New York, New York 10012;
and Département de Mathematics and Statistics, Université d'Ottawa, Ottawa, Ontario K1N 6N5, Canada

(Received 29 December 2005; accepted 28 July 2006; published online 3 October 2006)

The conditional dissipation and diffusion for a passive scalar with an imposed mean gradient are studied here. The results are obtained for an elementary model consisting of a random shear flow with a simple time-periodic transverse sweep. As the Peclet number is increased, scalar intermittency is observed; the scalar probability density function departs strongly from a Gaussian law. As a result, the conditional dissipation undergoes a transition from a quadratic behavior for the near-Gaussian probability distribution case at low Peclet number to a more complex shape at large Peclet. The conditional diffusion also undergoes a transition, this time from a linear to a nonlinear dependence, for cases with sufficient intermittency as well as a significant contribution from multiple spatial modes. The present analysis sheds some light on similar behaviors observed recently in numerical simulations of more complex models. The statistics in the present study are obtained by exact processing of one-dimensional quadrature results so that all sampling errors are eliminated, including in the tails of the distribution. This allows for a quantification of typical sampling errors when the conditional statistics are processed from numerical databases. The robustness of models based on polynomial fits for the conditional statistics is also assessed.
 [DOI: 10.1063/1.2353880]

I. INTRODUCTION

Intermittency is a key feature of turbulent flows and correctly taking it into account in turbulence models is of critical importance, albeit quite challenging. This is true not only for velocity fluctuations, but also for scalar variables such as the temperature, as demonstrated by the classical Chicago experiments[1–4] on Rayleigh-Benard convection, where non-Gaussian probability density functions (PDFs) were reported for the temperature fluctuations. Understanding the fundamental mechanisms that can potentially lead to such behavior is a question of great theoretical interest and has motivated a number of studies with a passive scalar advected by flows of various complexity.[5–12] That such complex intermittent behavior can be studied unambiguously via judiciously chosen idealized models has been demonstrated in Refs. 13–17 for the case of a decaying scalar at long times, and in Ref. 18 for the case of a scalar with a mean gradient. This latter case is now revisited to extend the study beyond that of the scalar PDF.

A recurring issue addressed in several of the studies cited above is to analyze and predict the behavior of the conditional statistics of the passive scalar fluctuations, in particular the conditional dissipation and the conditional diffusion. This is relevant both on the theoretical level as well as in the context of developing practical turbulence models for various applications. For example, on the theoretical level, an exact formula relating the shape of the PDF with the conditional dissipation and diffusion has been derived.[19,20] Understanding theoretically the behavior of those conditional statistics would therefore be one venue to approach the study of the scalar PDF, in particular its tails, for the nontrivial non-Gaussian case.[5,12,20] For instance, it has been suggested that, under some conditions, the conditional diffusion and dissipation could be adequately fitted by polynomials (linear and quadratic respectively, at least in the simplest cases),[7] as a result of which one could formulate a closure strategy for the scalar PDF in terms of a very limited number of parameters as well as predict the general behavior of the PDF's tails. An example from the practical modeling context is the flamelet closure approach in turbulent combustion, where models for the PDF and the conditional statistics play a key role. In such models (see, for example, Ref. 21 for an introduction), one relies on the asymptotic behavior of a thin flame to shortcut the very challenging issue of the direct turbulent closure for the nonlinear reaction term in the scalar equation. Instead, one expresses the reactive scalar as a function of an appropriate passive scalar and its derivatives, so that one obtains the large scale behavior for the reactive scalar by averaging the function of the passive scalar, weighted by the joint PDF of the passive scalar fluctuations and its conditional dissipation. Because of the nonlinear nature of such application, it is critical to capture adequately the effect of intermittency on the joint PDF tail behavior, as nonlinearity can magnify tremendously their impact on the global behavior of the solution.

Unfortunately, studying the conditional statistics by processing discrete databases, either experimental or numerical ones, can be an extremely challenging task as very limited data are statistically available in the tails of the PDF. Typical results are very noisy and make it quite challenging to extract definite trends for theoretical and modelling purposes.

In this paper, an idealized model[18] that leads to passive scalar intermittency is revisited, with the objective of analyzing the behavior of the passive scalar conditional statistics. The model is surprisingly simple: the ingredients for intermittency are the presence of a large scale gradient imposed on the scalar and a very simple advection flow with a steady or unsteady Gaussian random shear flow in one direction and a time-dependent, uniform in space, transverse sweep. Despite the simplicity of the model, PDF intermittency is observed; a summary of the key results of the PDF analysis is found in Sec. II. The solution for the passive scalar is obtained via Duhamel's formula. Practically, it involves solving numerically an ordinary differential equation and processing exactly that numerical solution. Explicit processing formulas for the conditional statistics are developed in Sec. III. The case of a single, steady mode is first analyzed in Sec. IV, where exact, numerical, and asymptotic results are presented. For that case, the conditional diffusion is trivially linear, as expected in the nonintermittent, Gaussian case. However, the conditional dissipation differs strongly from its Gaussian PDF case counterpart; the link with intermittency is identified explicitly. In Sec. V, the more practically relevant case of a multimode unsteady Gaussian random shear is studied. In that case, as the Peclet number is increased, both the conditional dissipation and the conditional diffusion show strongly non-Gaussian responses; in particular, the nonlinearity of the conditional diffusion is explained. Many of the observations in the idealized model studied here resemble qualitatively those in much more complex models,[7,10] but the conclusions, in particular, in the tails, are somewhat different. In Sec. VI, a study of sampling errors in the tails is performed, which can to some extent explain those differences in interpretation. In Sec. VII, strategies for polynomial fitting of the conditional statistics are revisited, in particular in the context of formulating simple closures for the scalar PDF.

II. IDEALIZED MODEL

A. Basic setup

In this section, we explain the setup for the idealized model and summarize the key results from Ref. 18 regarding the scalar fluctuation PDF. The model consists of the advection and diffusion of a passive scalar according to the following equation, in nondimensional form:

$$\frac{\partial Z}{\partial t} + \mathrm{Pe}(\mathbf{v}\cdot\nabla Z) = \Delta Z. \tag{1}$$

The nondimensionalization in Eq. (1) is completely standard. The spatial units are scaled using a prescribed large length scale L. Given the scalar diffusivity κ, the time scale is taken as the viscous time L^2/κ. The Peclet number is given by $\mathrm{Pe}=VL/\kappa$, where V is the typical magnitude of the velocity field. All length and time scales in this paper are expressed in those units. The problem is studied in two spatial dimensions, with longitudinal coordinate x and transverse coordinate y. The two-dimensional velocity field is a time-dependent shear flow with a transverse cross sweep, i.e.,

$$\mathbf{v} = (v(y,t), w(t)). \tag{2}$$

Here, $v(y,t)$ is deterministic or random, and

$$w(t) = \beta \sin(\omega t) \tag{3}$$

is a periodic function of time of period $\tau_P = 2\pi/\omega$. A key feature of this velocity field is that its longitudinal component $v(y,t)$ is an autonomous function of the transverse coordinate y, i.e., it is not swept by the transverse velocity. This is essential for the intermittent bursting mechanism described in the next section. We seek the statistically stationary solution of Eqs. (1) and (2), where a mean gradient is imposed along the x axis, i.e.,

$$Z = \frac{x}{L_g} + Z'(x,y,t), \tag{4}$$

where Z' is of mean zero. The mean gradient part x/L_g is a trivial solution to Eq. (1) when $\mathrm{Pe}=0$, so that $Z'(x,y,t)$ represents the perturbation in the scalar induced by the flow for nonzero Pe.

B. Key features of the solution

Before giving all the necessary technical details, we give here a qualitative summary of some key observations from Ref. 18. The model above has the following two important properties: the availability of explicit solution formulas and the richness of the underlying physics leading to highly nontrivial solutions. The key simplification pertaining to the solution to Eq. (1) with the specific flow in Eq. (2) is that Z' can be taken as a function of y and t alone. Developing this solution in Fourier modes in y further reduces the problem down to solving ordinary differential equations (details are given below regarding the reduction procedure and the corresponding explicit solution formulas). This is attractive numerically, as the computational effort is tremendously reduced compared to that of discretizing directly the partial differential equation in Eq. (1). It also allows an extensive theoretical asymptotic analysis of the solution properties. The surprising feature of the solution behavior is that despite the simplicity of the model, it leads to intermittency in its solution at large Pe, as denoted for example by the strong departure of the scalar PDF from a Gaussian distribution. It is the time modulation in the transverse sweep, more precisely the fact that the sweep crosses zero periodically, that leads to the intermittency. An intuitive explanation of that mechanism is as follows: when the transverse sweep is near zero, the longitudinal shear has a very large distorting effect on the scalar, so that mixing is tremendously enhanced, while when the transverse sweep is near its maximum amplitude, the fast sweeping quenches the mixing power of the shear, which becomes order of magnitude smaller than when the sweep is zero. The bursts of mixing associated with the zero-crossing of the sweep are the rare events leading to intermittency and non-Gaussian PDFs. In particular, the model illustrates that none of the following structural conditions are required for passive scalar intermittency: velocity fields with chaotic particle trajectories and at least one positive

Lyapunov exponent, many turbulent scales in the velocity field, statistical random fluctuations of at least one scale in the velocity field.

C. Explicit formulas for the scalar

Following Ref. 18, we assume the following expansion in spatial modes for $v(y,t)$

$$v(y,t)=\sum_J \hat{v}_J e^{iK_J y},$$
$$\hat{v}_J^*(t)=\hat{v}_{-J}(t) \quad \text{reality condition}, \tag{5}$$

where the amplitudes $\hat{v}_J(t)$ are considered for now to be steady statistically stationary complex Gaussian random fields in time (see the spatio-temporal case below). For that type of flow, the statistically stationary solution $Z'(y,t)$ is given by the related expansion:

$$Z'(y,t)=\frac{\mathrm{Pe}}{L_g}\sum_J \widehat{Z}'_J e^{iK_J y} \quad \text{with } \overline{\widehat{Z}'_J(t)}=\widehat{Z}'_{-J}, \tag{6}$$

where $\widehat{Z}'_J$ satisfies the following linear inhomogeneous ordinary differential equations:

$$\frac{d\widehat{Z}'_J}{dt}+(K_J^2+iK_J\,\mathrm{Pe}\,w(t))\widehat{Z}'_J=-\hat{v}_J.$$

The solution for $\widehat{Z}'_J$ can be obtained via Duhamel's formula to yield the following explicit formula for the stationary solution:

$$Z'(y,t)=\frac{\mathrm{Pe}}{L_g}\sum_J \widehat{Z}'_J(t)e^{iK_J y}$$
$$\text{with} \quad \widehat{Z}'_J(t)=-\int_{-\infty}^{t} S_{K_J}(t,t')\hat{v}_J(t')dt', \tag{7}$$

where S_{K_J} is the explicit solution operator:

$$S_{K_J}(t,t')=e^{-K_J^2(t-t')}e^{-iK_J\mathrm{Pe}\int_{t'}^{t}w(s)ds}. \tag{8}$$

For a more general case for the velocity field, we assume now that the random Fourier amplitudes in $\hat{v}_J(t)$ have the form[22]

$$\hat{v}_J(t)=\tfrac{1}{2}(\eta_J(t)-i\xi_J(t)), \quad J>0,$$
$$\hat{v}_{-J}(t)=\tfrac{1}{2}(\eta_J(t)+i\xi_J(t)), \tag{9}$$

where $\eta_J(t)$ and $\xi_J(t)$ are real Gaussian random fields which are independent from each other and also independent for $J\neq J'$ with covariance $R_J(|t|)$ given by

$$\langle \eta_J(t+t_0)\,\eta_J(t_0)\rangle_v=\langle \xi_J(t+t_0)\xi_J(t_0)\rangle_v=R_J(|t|). \tag{10}$$

We further assume that the time dependence is characterized by the correlation time τ_J, so that the covariance can be written as

$$R_J(|t|)=E_J e^{-|t|/\tau_J}, \tag{11}$$

where E_J is the shear energy at mode K_J, and the scalar $Z'(y,t)$ is also a Gaussian random variable, obtained as a superposition of Gaussian random modes $\widehat{Z}'_J(t)$ whose variances $\sigma_J^2(t)$ are obtained using a generalization of Duhamel's formula (7)

$$\sigma_J^2(t)=\frac{\mathrm{Pe}^2}{L_g^2}\int_{-\infty}^{t}\int_{-\infty}^{t} S_{K_{-J}}(t,t')S_{K_J}(t,\tilde{t})R_J(|t'-\tilde{t}|)dt'd\tilde{t}, \tag{12}$$

where

$$\sigma_J^2(t)=\langle|\hat{Z}'_J(t)|^2\rangle_v.$$

D. Scalar PDF behavior

Based on these solution formulas, one can now obtain an explicit processing procedure to extract the scalar fluctuations PDF. First, one introduces the partial PDF, $p_{Z'(y,t)}$, which is the PDF at a fixed time, after averaging over the velocity fluctuations. As a result of the analysis above, it is clear that this partial PDF is also necessarily a Gaussian distribution, independent of y and given explicitly by the formula

$$p_{Z'(t)}(\lambda)=\frac{1}{\sqrt{2\pi}\sigma(t)}e^{-\lambda^2/2\sigma^2(t)}=\frac{1}{\sigma(t)}G\left(\frac{\lambda}{\sigma(t)}\right),$$
$$\sigma^2(t)=\langle|Z'(t)|^2\rangle_v \tag{13}$$

with $G(\lambda)=(2\pi)^{-1/2}\exp(-\lambda^2/2)$ the normalized Gaussian. The partial scalar variance $\sigma^2(t)$ is an explicit periodic function of time which is readily calculated through the formulas in (7) or (12). Once the partial PDF is known, the full PDF is simply obtained by averaging over time

$$p_{Z'}=\frac{1}{\tau_P}\int_0^{\tau_P} p_{Z'(t)}dt.$$

One should remark that, even though the partial PDF is necessarily Gaussian in the present model, this is not always the case for the full PDF. Indeed, it was shown in Ref. 18, that, at low Pe, $\sigma^2(t)$ varies very little within the time period, and the full PDF is nearly Gaussian, but as Pe is increased, there are intermittent bursts in the solution for $\sigma^2(t)$, which lead to a strongly non-Gaussian PDF with fat tails.

III. EXPLICIT FORMULAS TO PROCESS THE CONDITIONAL STATISTICS

A. Definitions

(From now on, for simplicity, we drop the prime and write Z instead of Z'.) We rewrite Eq. (6) as

$$Z(y,t)=\Sigma_J[A_J(t)\sin K_J y+B_J(t)\cos K_J y],$$

where A_J, B_J follow a Gaussian distribution, with mean zero, and variance $\sigma_J^2(t)$ obtained as explained in the previous section.

With that notation, the derivative of Z with respect to y is given by

$$Z_y(y,t) = \Sigma_J K_J [A_J(t)\cos K_J y - B_J(t)\sin K_J y]$$

with the direct consequence that, as was the case for PDF of $Z(y,t)$, the partial PDF of $Z_y(y,t)$ at a given fixed time t is also Gaussian, with mean zero, independent of y, and with variance $\Sigma_J K_J^2 \sigma_J^2(t)$. Similarly, the second derivative of Z with respect to y is given by

$$Z_{yy}(y,t) = -\Sigma_J K_J^2 (A_J(t)\sin K_J y + B_J(t)\cos K_J y)$$

with the consequence that the partial PDF of Z_{yy} is also Gaussian, with mean zero, independent of y, and with variance $\Sigma_J K_J^4 \sigma_J^2(t)$.

The conditional dissipation $G(Z)$ is defined as

$$G(Z) = \langle Z_y^2 | Z \rangle_{\tau_P, v}. \tag{14}$$

Similarly, the conditional diffusion $D(Z)$ is defined as

$$D(Z) = \langle Z_{yy} | Z \rangle_{\tau_P, v}. \tag{15}$$

Both conditional statistics above are obtained by averaging with respect to both the velocity fluctuations and the time. As in the case of the PDF of the passive scalar fluctuations, it is convenient to introduce the partial conditional dissipation $G(Z,t)$ and diffusion $D(Z,t)$, defined, respectively, as

$$G(Z,t) = \langle Z_y^2 | Z \rangle_v, \tag{16}$$

$$D(Z,t) = \langle Z_{yy} | Z \rangle_v, \tag{17}$$

i.e., obtained by averaging solely over the velocity statistics, but not over time. Then the global conditional dissipation $G(Z)$ and diffusion $D(Z)$ are obtained very easily according to the appropriate time-weighted average

$$G(Z) = \frac{\frac{1}{\tau_P}\int_{\tau_P} G(Z,t)\,\mathrm{pdf}(Z(t))dt}{\frac{1}{\tau_P}\int_{\tau_P} \mathrm{pdf}(Z(t))dt} = \frac{\frac{1}{\tau_P}\int_{\tau_P} G(Z,t)\,\mathrm{pdf}(Z(t))dt}{\mathrm{pdf}(Z)}, \tag{18}$$

$$D(Z) = \frac{\frac{1}{\tau_P}\int_{\tau_P} D(Z,t)\,\mathrm{pdf}(Z(t))dt}{\frac{1}{\tau_P}\int_{\tau_P} \mathrm{pdf}(Z(t))dt} = \frac{\frac{1}{\tau_P}\int_{\tau_P} D(Z,t)\,\mathrm{pdf}(Z(t))dt}{\mathrm{pdf}(Z)}. \tag{19}$$

Note that the weight $\mathrm{pdf}(Z(t))$ needed in those conditional averages will play an important role. For instance, we will see that $G(Z,t)$, the conditional dissipation at a fixed time, is independent of Z, but not $G(Z)$, as a consequence of the weighted time-averaging. Similarly, the partial conditional diffusion $D(Z,t)$ in the present setup is always a linear function of Z, but because of the weighted time-averaging, it will be shown that the global conditional diffusion $D(Z)$ is not, at least in the multimode case.

B. Preliminary formulas for the partial conditional statistics

According to the previous sections, the distributions at a fixed time t for $Z(y,t)$, $Z_y(y,t)$, and $Z_{yy}(y,t)$ are all linear combinations of Gaussian distributions $A_J(t)$ and $B_J(t)$. We summarize here basic results regarding the conditional statistics for such combinations.

Let $Y=[Y_1, Y_2, \ldots, Y_n]' = N(0,\Sigma)$ be an n by 1 vector with Gaussian distribution, of mean zero and variance matrix $\Sigma = \mathrm{diag}(\sigma_1^2, \sigma_2^2, \ldots, \sigma_n^2)$. Let us consider two general linear combinations X_1 and X_2 of Y, where $X_1 = a_1' Y$ and $X_2 = a_2' Y$, where the respective weight distributions are $a_1 = [a_{11}, a_{12}, \ldots, a_{1n}]'$, $a_2 = [a_{21}, a_{22}, \ldots, a_{2n}]'$. This can be rewritten as $X = [X_1, X_2] = A'Y$ with $A = [a_1, a_2]$ a matrix of size $n \times 2$.

A first elementary statistical result is that the distribution of X is a normal distribution, with mean zero and variance $A'\Sigma A$:

$$L(X) = N(0, A'\Sigma A).$$

The explicit expression for the distribution of the value of X_1 conditioned on X_2 is given by

$$L(X_1|X_2) = N\left(\frac{a_1'\Sigma a_2}{a_2'\Sigma a_2} X_2, \sigma_{11,2}^2\right), \tag{20}$$

where

$$\sigma_{11,2}^2 = a_1'\Sigma a_1 - \frac{(a_1'\Sigma a_2)^2}{a_2'\Sigma a_2}. \tag{21}$$

This result will be useful to compute the partial conditional diffusion. Similarly, the expression for the distribution of X_1^2 conditioned on X_2 is given by

$$L(X_1^2|X_2) = \sigma_{11,2}^2 \chi^2\left(\frac{a_1'\Sigma a_2}{a_2'\Sigma a_2} X_2\right). \tag{22}$$

In particular, if $a_1'\Sigma a_2 = 0$, then the last distribution is the centered χ^2 and X_1 and X_2 are independent. This formula will be used in the next section to compute the partial conditional dissipation of Z.

IV. CONDITIONAL STATISTICS FOR THE SINGLE MODE CASE

A. Explicit formulas

We first apply the general conditional statistics formulas from the previous section to the case of a single mode J, so that

$$Z = A_J \sin K_J y + B_J \cos K_J y,$$

$$Z_y = K_J(A_1 \cos K_J y - B_J \sin K_J y),$$

$$Z_{yy} = -K_J^2(A_J \sin K_J y + B_J \cos K_J y).$$

By simple inspection, it is clear that $Z_{yy}=-K_J^2 Z$, so that the partial conditional diffusion and the conditional diffusion are trivial: $D(Z,t)=D(Z)=-K_J^2 Z$. It is always linear (unlike what will happen in the multimode case, as discussed in the next section).

To obtain the partial conditional dissipation, we use Eq. (22) with $a_1=[K_J \cos K_J y, -K_J \sin K_J y]'$, $a_2=[\sin K_J y, \cos K_J y]'$, and $\Sigma=\mathrm{diag}(\sigma_J^2(t),\sigma_J^2(t))$.

Plugging into the formula, one finds that the distribution of Z_y^2 conditioned on Z at a fixed time is independent of Z:

$$L(Z_y^2(t)|Z,t) = K_J^2 \sigma_J^2(t) \chi^2(0). \tag{23}$$

The average of that distribution with respect to the velocity statistics is the partial conditional dissipation

$$G(Z,t) = \langle L(Z_y^2(t)|Z,t)\rangle_{v'} = K_J^2 \sigma_J^2(t) \langle \chi^2(0)\rangle = K_J^2 \sigma_J^2(t)$$

so that the (global) conditional dissipation is given by

$$G(Z) = K_J^2 \frac{\dfrac{1}{\tau_P}\displaystyle\int_0^{\tau_P} \sigma_J^2(t)\,\mathrm{pdf}_g(Z;0,\sigma_J(t))dt}{\mathrm{pdf}(Z)}. \tag{24}$$

One remarks that, because of the weighted averaging, the conditional dissipation is now a function of Z, even though the partial conditional dissipation at the fixed time t was only a function of time, not of Z. Also, direct inspection of the formula gives an upper-bound for the conditional dissipation: $G(Z) \le K_J^2 \max_t(\sigma_J^2(t))$.

B. Asymptotic formula in the large Pe self-similar regime

We consider here the case of a stationary single mode Gaussian shear flow. The detailed analysis of the self-similar regime both for the steady and unsteady cases can be found in Ref. 18. The condition for self-similarity is that Pe be sufficiently large such that $\tau_P K_J^2 (1+1/\tau_J)^2 < \mathrm{Pe}\,\beta$. If that condition is satisfied, stationary phase asymptotics gives the following expression for $\sigma_J^2(t)$:

$$\sigma_J^2(t) = \sigma_{J,\max}^2 e^{-2K_J^2 t} \quad \text{with } \sigma_{J,\max}^2 = \frac{\mathrm{Pe}\,\tau_P}{K_J L_g^2 \beta} \tag{25}$$

for $0 \le t \le \tau_P/2$ (periodic continuation for other t). The small Z behavior (inner core around $Z=0$) is obtained by substituting this expression for $\sigma_J^2(t)$ in Eqs. (13) and (24) and expanding for small Z:

$$G(Z) = \sigma_{J,\min}\sigma_{J,\max} + (1/\sigma_{J,\min}^2 - 1/\sigma_{J,\max}^2)^2 Z^2 + \cdots.$$

This demonstrates the effect of intermittency on the conditional dissipation. At low Pe, the variance $\sigma_J^2(t)$ is nearly constant and so is the conditional dissipation. As Pe increases however, the difference between $\sigma_{J,\min}$ and $\sigma_{J,\max}$ increases, and curvature at the origin increases. This could explain the type of behavior observed for instance in Refs. 9 and 10, where the conditional dissipation in the numerical experiments displayed this type of transition. This asymptotic prediction will be confirmed next by numerical results.

For large Z values, one can show that the asymptotic upper bound is actually achieved, so that

$$\lim_{Z\to\infty} G(Z) = K_J^2 \sigma_{J,\max}^2.$$

C. Numerical results

The numerical results are obtained by exact processing of $\sigma_J^2(t)$ according to (24). The time evolution of $\sigma_J^2(t)$ could be obtained via Duhamel's formula (7). For practical purposes, it is however simpler to directly integrate numerically the ordinary differential equations to compute the Fourier modes amplitudes of the solution. The numerical integration is performed with Matlab ode15s, an adaptive high order integrator that can handle stiff problems. This numerical strategy exploits the special structure of the solution to reduce the numerical complexity by several orders of magnitude compared to the direct numerical simulation of the unsteady two-space dimension PDE for the passive scalar. In particular, the time-integration of the Fourier modes amplitudes can be made arbitrarily accurate at reasonable cost. Moreover, because in the present problem, explicit processing formulas for the conditional statistics are available, there is no sampling error. In general, in the absence of such explicit formula, lack of data in the tails of the PDF can cause severe accuracy limitations for the conditional statistics there. All the test-cases reported next correspond to $\beta=1$ and $\omega=2\pi$ (so that $\tau_P=1$).

The first set of test cases corresponds to a single steady mode ($K_J=2\pi$, $1/\tau_J=0$). The corresponding results in Fig. 1 confirm the theoretical predictions. In that plot, and all similar subsequent plots, the standard normalization is used, i.e., Z is rescaled by its standard deviation $\bar{\sigma}_J=\sqrt{\bar{\sigma}_J^2}$ where the variance is computed as $\bar{\sigma}_J^2=\langle\sigma_J^2(t)\rangle_{\tau_P}$. The conditional dissipation is normalized by the mean dissipation $K_J^2\bar{\sigma}_J^2$. The conditional diffusion is normalized by $K_J^2\bar{\sigma}_J$, so that the single mode linear profile has a slope of -1 in the normalized units. As expected from the discussion above, the conditional dissipation shows a quadratic inner core around $Z=0$ that shrinks as Pe is increased. Out in the tails, the conditional dissipation saturates at the predicted limit value for large Z. In the renormalized units, this limit value is given by $\sigma_{J,\max}^2/\bar{\sigma}_J^2$. As Pe increases, the saturation is achieved further out in the tails. The large Pe, large Z, asymptotic trend is shown more clearly in Fig. 2, where the results for Pe=10000 (circles) are shown along with the large Pe asymptotic prediction over a very wide range of values for Z of plus or minus 40 standard deviations. Averaging Eq. (25) over the half time-period, one obtains that the nondimensionalized saturation value for the conditional dissipation in the limit of large Z, large Pe, is given by $\sigma_{J,\max}^2/\bar{\sigma}_J^2 \to K_J^2\tau_P$. This is indeed the value observed in Fig. 2, where the predicted asymptotic saturation value is shown as a dashed line.

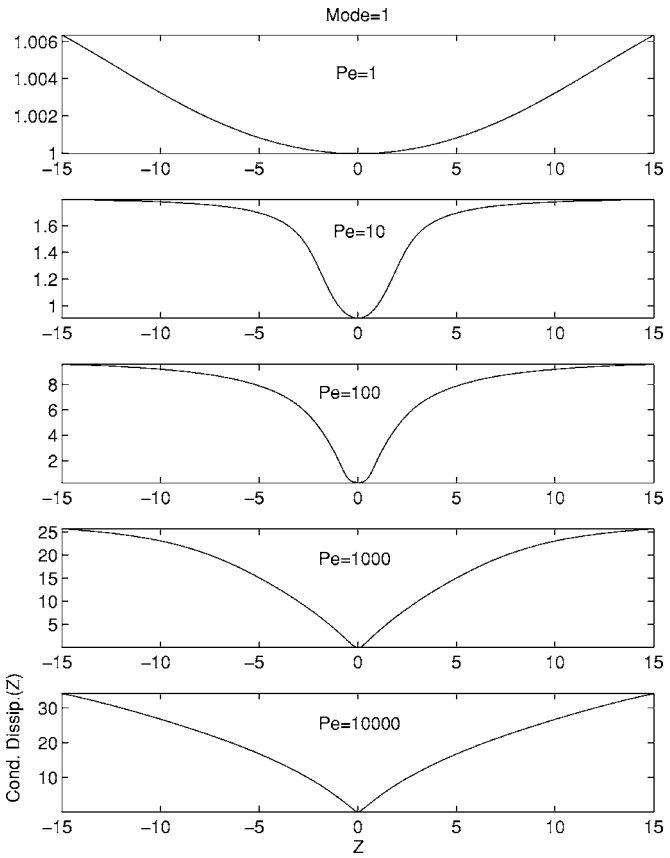

FIG. 1. Conditional dissipation, single steady mode, $K_1=2\pi$, various Pe.

The second set of test cases corresponds again to a single steady mode, this time at the fixed value of Pe=1000, for various modes J with $K_J=2J\pi$. The results are presented in Fig. 3. Based on the analysis in Ref. 18, increasing K_J will eventually lead to a more Gaussian scalar PDF. According to the analysis above, this means that as K_J increases, the conditional dissipation should display less variation between its largest and smallest values (respectively, for Z large and near zero). At the same time, the inner quadratic core should expand. This is indeed observed in the numerical results.

The final set of test cases in this section focusses now on the unsteady single mode case. Pe=1000 and $K_J=2\pi$ are fixed and τ_J is progressively decreased down from its value

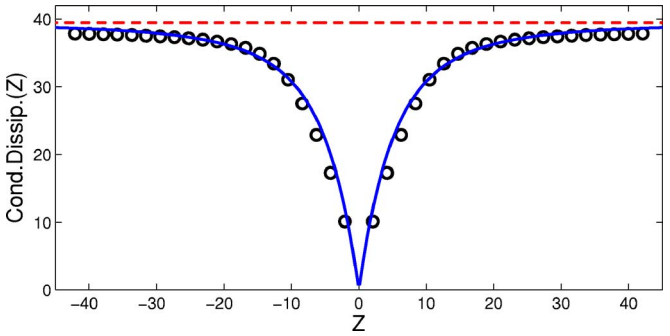

FIG. 2. Conditional dissipation, single steady mode, $K_1=2\pi$. Solid line: asymptotic prediction for Pe$\to\infty$; circles: case Pe=10000; dashed line: asymptotic prediction for the large Z, large Pe saturation level.

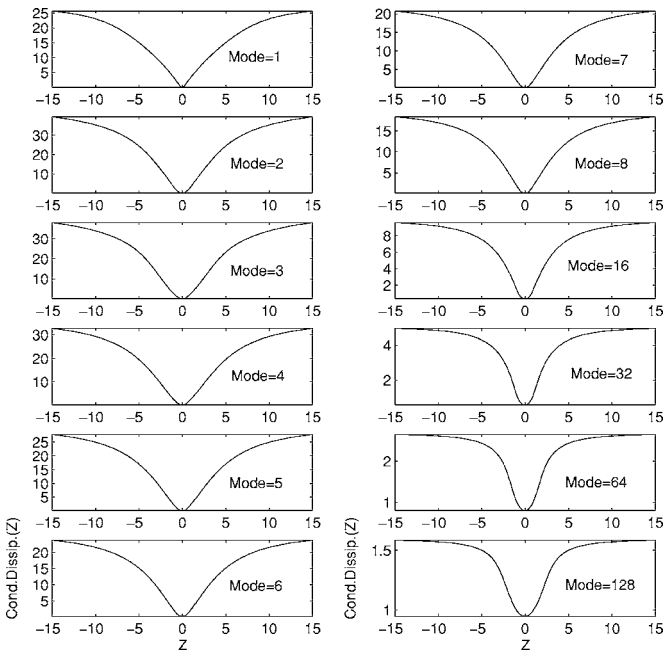

FIG. 3. Conditional dissipation, single steady mode, Pe=1000, various shear spatial frequencies $K_J=2J\pi$.

in the steady case, where $1/\tau_J=0$. It is known (see Ref. 18 for the application to the present context) that decreasing the correlation time τ_J leads to a more Gaussian scalar PDF (the limit of the δ correlation in time is an exactly Gaussian PDF). According to the analysis above, this means that as $\tau_J\to 0$, the conditional dissipation should display less variation between its largest and smallest values (respectively, for Z large and near zero). At the same time, the inner quadratic core should become more visible. This is precisely what is observed in the numerical results in Fig. 4.

Remark: All the results presented here correspond to the fixed values $\tau_P=1$ and $\beta=1$. Other interesting approaches to the asymptotic limit and a variety of regime transitions could be observed by fixing other parameters, τ_J for instance, and letting τ_P or β vary.

V. CONDITIONAL STATISTICS: MULTIMODE CASE

A. Explicit formulas

Similarly to the single mode case, the partial conditional dissipation at a fixed time t is given by

$$G(Z,t)=\Sigma K_J^2\sigma_J^2(t)$$

and the conditional dissipation is obtained by properly averaging with respect to time according to (18):

$$G(Z)=\Sigma\frac{\frac{1}{\tau_P}\int_0^{\tau_P}K_J^2\sigma_J^2(t)\mathrm{pdf}_g(Z;0,\Sigma\sigma_J(t))dt}{\mathrm{pdf}(Z)}. \tag{26}$$

Just as in the single mode case, at a fixed time t, the partial conditional dissipation is independent of Z, but this is not the case for the full conditional dissipation. Processing now the formulas for the conditional diffusion, the partial diffusion

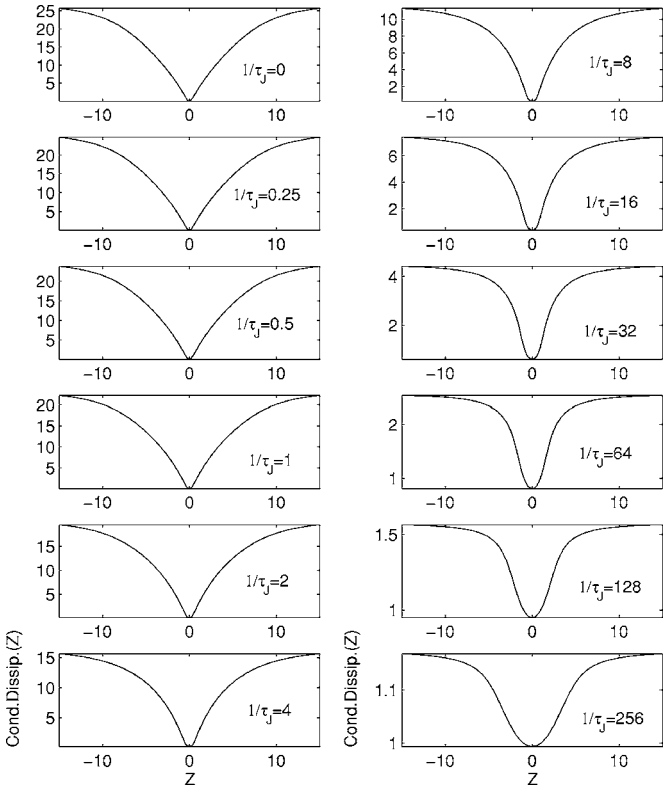

FIG. 4. Conditional dissipation, single mode, unsteady case, Pe=1000, $K_J=2\pi$, various correlation times τ_J.

distribution can be obtained using Eq. (20), with the following result at time t:

$$L(Z_{yy}|Z)=N\left(-\frac{\Sigma K_J^2\sigma_J^2(t)}{\Sigma\sigma_J^2(t)}Z,\Sigma K_J^4\sigma_J^2(t)-\frac{(\Sigma K_J^2\sigma_J^2(t))^2}{\Sigma\sigma_J^2(t)}\right).$$

If there is only one mode, the variance is zero and one recovers the single mode formula. The partial conditional diffusion at time t is the mean of this distribution

$$D(Z,t)=-\frac{\Sigma K_J^2\sigma_J^2(t)}{\Sigma\sigma_J^2(t)}Z.$$

As in the one mode case, the partial conditional diffusion is a linear function of Z, but the slope is now a nonlinear function of time. The conditional diffusion is obtained by the properly weighted time integral of that expression:

$$D(Z)=-\frac{\frac{1}{\tau_P}\int_0^{\tau_P}\frac{\Sigma K_J^2\sigma_J^2(t)}{\Sigma\sigma_J^2(t)}\mathrm{pdf}(Z(t))dt}{\mathrm{pdf}(Z)}Z. \quad (27)$$

Unlike the single mode case, this is clearly a nonlinear expression with respect to Z.

B. Numerical results

The numerical simulations for the random spatio-temporal multimode shear case are performed by assuming an energy spectrum for the velocity of the form

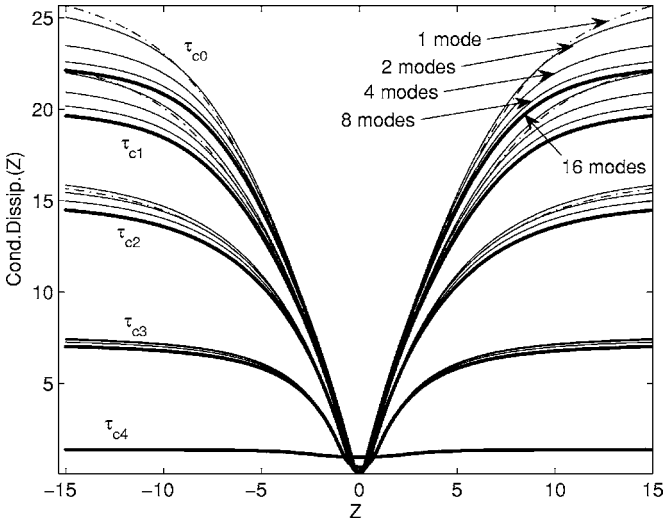

FIG. 5. Conditional dissipation, multimode unsteady case, Pe=1000, effect of the number of modes in the energy spectrum for various correlation times τ_J.

$$E_J\propto K_J^{-\alpha} \quad (28)$$

for modes $K_J=2\pi\{1,2,\ldots,N\}$. The simulation results presented here correspond to $\alpha=1$ (Batchelor spectrum), but other choices are possible, for example, $\alpha=5/3$ (Kolmogorov spectrum). The correlation time of each mode is also expressed by a power law, with large values of K_J corresponding to shorter correlation times

$$\tau_J=\tau_C K_J^{-1} \quad (29)$$

with $\tau_C>0$ the correlation time constant.

The figures to be presented next use different numbers of modes ($N=1,2,4,8,16$) in combination with different correlation time constants ($1/\tau_{C0}=0$, $1/\tau_{C1}=2\pi$, $1/\tau_{C2}=8\pi$, $1/\tau_{C3}=32\pi$, $1/\tau_{C4}=1000$). Again, in those figures, all variables are properly nondimensionalized. Z is normalized by its standard deviation $\bar{\sigma}=\sqrt{\Sigma\bar{\sigma}_J^2}$. The conditional dissipation is normalized by the mean dissipation $\Sigma K_J^2\bar{\sigma}_J^2$. The conditional diffusion is normalized by $\Sigma K_J^2\bar{\sigma}_J^2/\bar{\sigma}$, so that the Gaussian PDF case corresponds to a linear profile for the conditional diffusion with a slope of −1 in the normalized units.

In Fig. 5, the conditional dissipation resembles qualitatively the corresponding curve for the single mode case. The limit of $1/\tau_C\to 0$ should lead to a Gaussian PDF so that the conditional dissipation should tend to a constant. This is observed here for τ_{C4}. The Gaussian limit is also reached by considering modes with very high wave numbers. As a consequence, when modes are combined according to the spectrum above, including an increasingly larger number of modes decreases the intermittency and the conditional dissipation flattens out, which is also observed here, for each value of τ_C, going from one up to 16 modes. The next two figures show the conditional diffusion for various combinations of τ_C and number of modes N.

In Fig. 6, the plots are grouped according to the value for τ_C. The linear conditional diffusion profile expected for the Gaussian PDF case is observed as predicted for the case of a

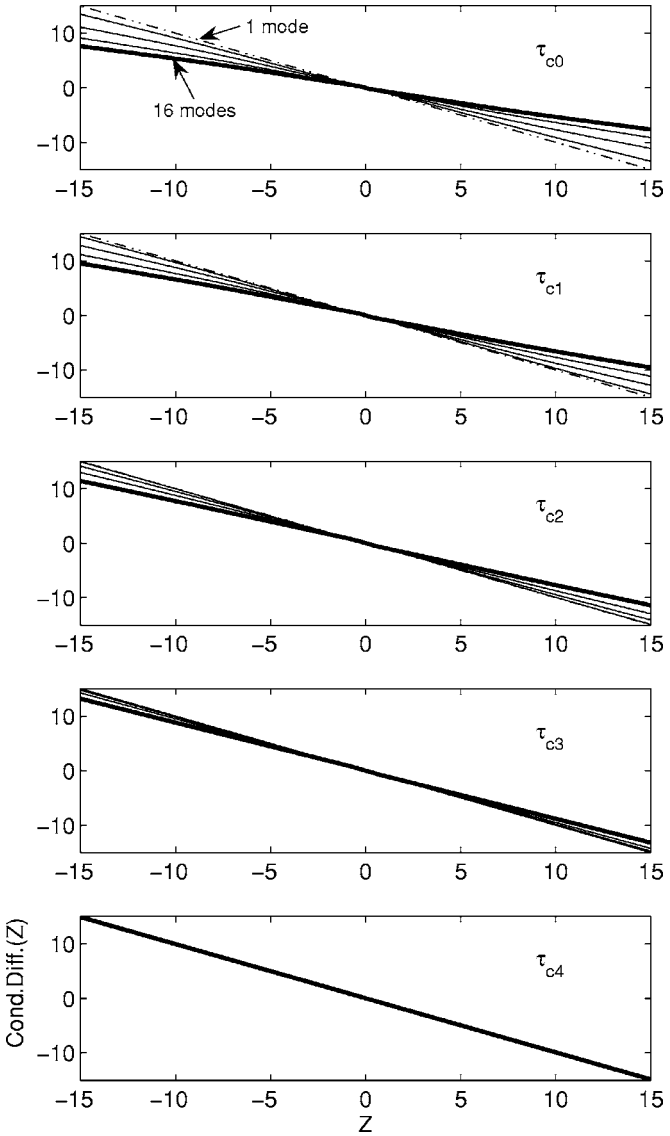

FIG. 6. Conditional diffusion, same as for Fig. 5.

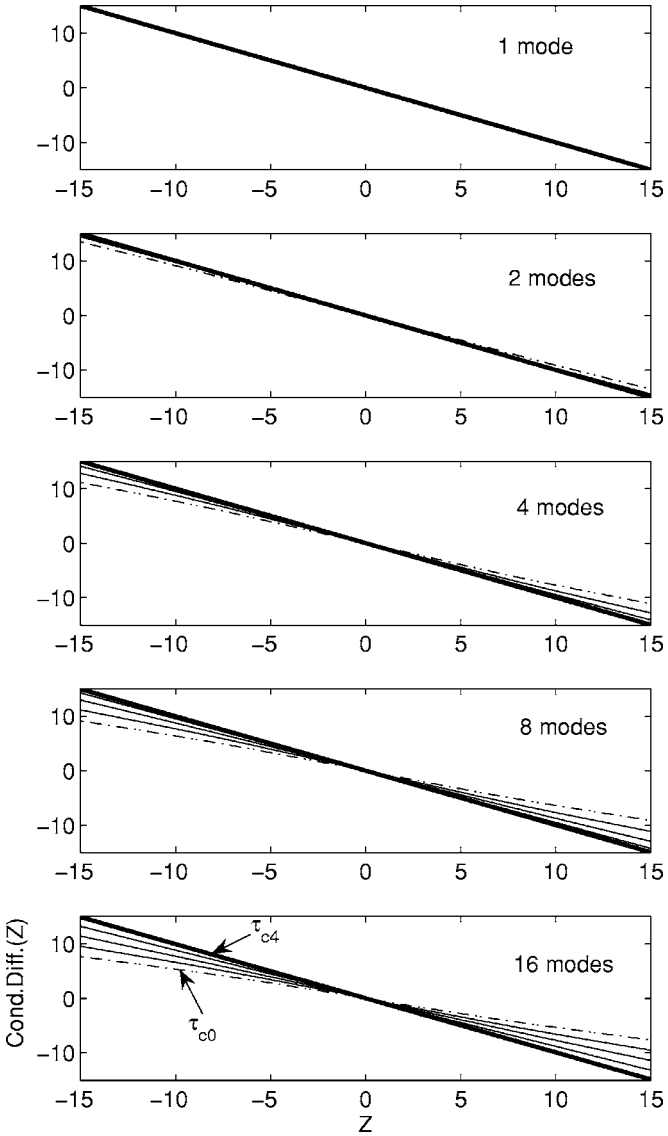

FIG. 7. Conditional diffusion, same as Fig. 5; effect of the correlation time τ_J for various numbers of modes in the energy spectrum.

the very large τ_{C4}. The effect of varying the number of modes is best seen in Fig. 7, where the same results are presented, this time grouped according to the number of modes. As expected, the one-mode case gives a perfectly linear profile, but as the number of modes is increased, the nonlinearity increases, with the slope becoming smaller as Z increases compared to the slope at $Z=0$.

VI. SAMPLING ERRORS IN THE PDF TAILS

In this section, we use the asymptotic limit of the conditional dissipation to study the potential impact of sampling errors in the tails of the PDF. As indicated in Eq. (23), the entire conditional distribution of the dissipation is known. The focus so far has been on its mean, the conditional dissipation. Its variance however plays a key role in quantifying the sampling error via the central limit theorem. We mimic here the process of extracting conditional statistics from a discrete database with N sampled points.

(1) In the practical procedure, the data points are gathered in n bins. We assume here that the bins have identical width Δz and cover the range $-15\bar{\sigma} \leq Z \leq 15\bar{\sigma}$. We mimic the binning process by estimating the number of points N_i in the bin $[zi-\Delta z/2, zi+\Delta z/2]$ as $N_i \sim N\int_{zi-\Delta z/2}^{zi+\Delta z/2} \mathrm{pdf}(z)dz$.
(2) Using the central limit theorem, the standard error of the mean based on a sample of N_i data points with standard deviation σ_i is $\sigma_i/\sqrt{N_i}$.

In Fig. 8, we show the plot of the conditional dissipation corresponding to the asymptotic solution along with the 95% confidence interval of $\pm 1.96\sigma_i/\sqrt{N_i}$. The plot corresponds to the single steady mode case, with $K_J=2\pi$, For this computation, we assumed that $N=10^6$ data points were available, and that $\Delta z=0.1$ so that 300 bins were used. The growth of the confidence interval in the tails is noticeable. It is due to the combination of two effects: the number of data points N_i for bins in the tails of the PDF becomes smaller, because the

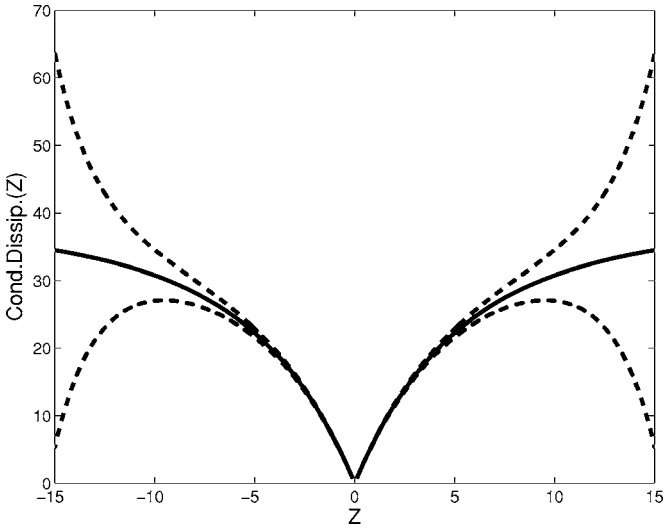

FIG. 8. Asymptotic conditional dissipation along with 95% confidence interval for its estimation based on data sampling.

PDF decreases; also, the standard deviation of the conditional distribution of the dissipation grows as Z grows. This explains the magnitude of the statistical noise observed frequently when processing conditional statistics, see for example, Fig. 10 in Ref. 5, Fig. 2 in Ref. 7, or Fig. 5 in Ref. 11. In particular, a linear or quadratic growth has been proposed for the conditional dissipation for large Z,[7,11] also see next section. In the present model however, the conditional dissipation tapers off to the limit value of $K_J^2\tau_P$ when Z becomes large (see Fig. 2). One might question whether the excessive noise in the data for the conditional dissipation at large Z in those previous experiments could mask such tapering for those cases also. One major advantage of the analysis presented in this paper is that sampling errors played no role; instead, explicit processing guarantees uniform accuracy in the processed statistics for an unlimited range of values for the passive scalar.

VII. PDF MODELING VIA POLYNOMIAL FITTING OF CONDITIONAL STATISTICS

For the class of stationary homogeneous random scalar PDFs such as the ones studied here, there is a well known formula relating the PDF, and the corresponding conditional dissipation and diffusion, see for example,[23,24,19]

$$\mathrm{pdf}(Z) = \frac{C}{G(Z)} \exp\left(\int_0^Z \frac{D(z')}{G(z')} dz' \right), \tag{30}$$

where C is a normalizing constant. There is no approximation involved in that equation, and it has indeed been verified using experimental or numerical data for the conditional dissipation and diffusion in the formula to reconstruct the PDF, and comparing this reconstructed PDF with the observed one, see Refs. 5 and 20, for example. This formula has also been considered in the context of designing a modeling strategy for the PDF, in particular its tails. Let us assume for the sake of simplicity that the conditional diffusion $D(z)$ is a linear function of Z (for our model, it is always the case if only one spatial mode is present). Then, Eq. (30) would give a precise description of the tails of the PDF if a useful exact formula for the conditional dissipation was available. One proposed strategy to obtain such a formula is to fit the conditional dissipation by a polynomial of appropriate degree and substitute that polynomial in the integral above.[5,7,19,20] Mostly quadratic fits were used for the conditional dissipation in those experiments. As noted before, this is indeed the most natural choice for the inner core of the conditional dissipation in our model, in particular at low or moderate turbulence level. Agreement between the reconstructed and the observed PDFs is typically fairly good for a range of values for Z on the order of four standard deviations. Outside that range, data for the PDF and for the conditional dissipation are typically too noisy to reliably assess the performance of the strategy. Next, we carry on that validation of this approach for our elementary test-case. Since there is no sampling or discretization errors associated with our analysis, a reliable validation can now be performed for a much wider range of values for Z. The results are presented in Fig. 9. The setup for the experiments involves a flow field with a single steady mode, for various Pe. The conditional dissipation is shown on the left. The circles correspond to the actual data points. The dashed line is the best quadratic fit, based on the inner-core, and the solid line is the best linear fit in the intermediate range, outside the inner-core. The corresponding PDFs are shown on the right: again, the PDF data from the direct computations are shown as circles. The PDFs obtained

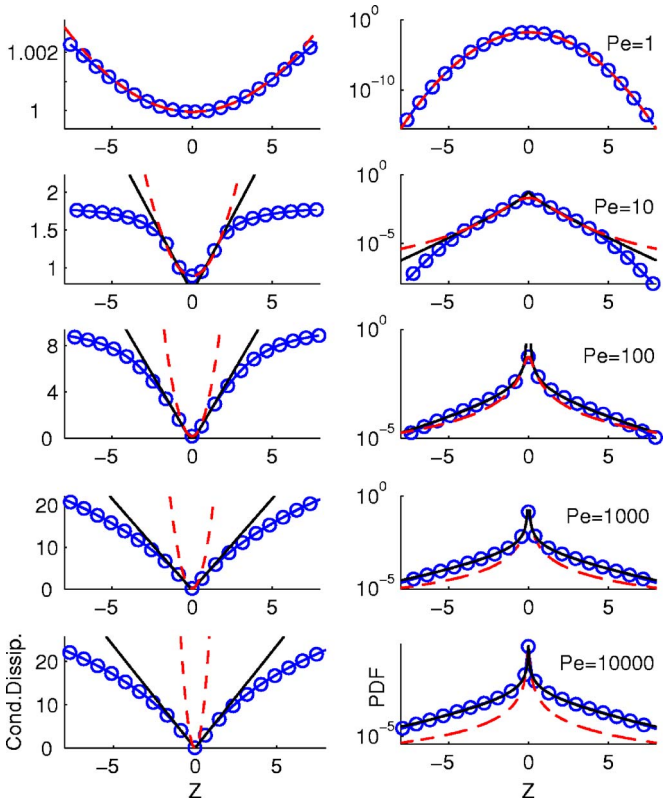

FIG. 9. Conditional dissipation (left) and exact and reconstructed PDFs (right) for various Pe, single mode steady case. Circles: numerical simulation data; solid line: linear fit of the conditional dissipation and corresponding reconstructed PDF; dashed line: quadratic fit.

using the quadratic fits are shown as dashed lines. At Pe=1, the PDF is actually nearly Gaussian, and the fit is perfect across the range of plus or minus eight standard deviations. As the Pe number is increased, the quadratic fit for the conditional dissipation agrees with the real data points over an increasingly narrow range of about two standard deviations at Pe=10, down to one standard deviation at Pe=100, and even smaller for Pe=1000,10000. Not surprisingly, the PDFs obtained by integrating Eq. (30) agree with the exact PDFs for about the same ranges of values for Z. In an attempt to increase that range, a procedure is used where the polynomial fit switches from quadratic to linear, for some transition value for Z in the intermediate range. The solid line in the PDF plots shows the results obtained after experimenting with the switching value, until an optimal value is identified, defined as the value for which one observes the largest range of values of Z with reasonable agreement between reconstructed and exact PDFs (this optimization is feasible here only because the exact PDF is available for comparison). With that strategy, it seems that the range of values of Z for which the reconstructed PDFs reasonably match the exact PDFs is actually surprisingly somewhat larger that the range over which the actual linear fit matches the conditional dissipation. Still, it is clear from the plots for $\mathrm{Pe} \geq 100$ that the tails behavior is not quite captured by the reconstruction procedure, even with this optimal choice. In conclusion, the reasonable agreement previously observed in other experiments between reconstructed and exact PDFs is confirmed, at small Pe or for a limited range of values of Z at moderate Pe. However, as far as the tails of the PDFs at large Pe are concerned, there seems to be no clear advantage to first model the conditional dissipation and then reconstruct from that model the PDF, rather to directly model the PDF itself. In addition, for more general setups, the nonlinearity of the conditional diffusion would need modelling also, further complicating the task at hand.

VIII. CONCLUSIONS

An elementary model that leads to scalar intermittency in PDFs has been revisited to study the behavior of the corresponding conditional dissipation and conditional diffusion. Typical experiments with more complex setups—numerical or physical—must deal with the noisiness of the data in the PDFs tails. On the other hand, the model here has no such limitations as it uses exclusively exact processing formulas applied to the results from elementary quadratures, so that reliable results are available, even in the tails of the PDFs. This has allowed for an extensive investigation of the conditional statistics and various related modeling issues, for a wide range of values of the passive scalar, including the tails of the PDFs. Quantitative explanations are proposed for some of the behaviors observed previously in more complex setups. For instance, the link between intermittency and the shape of the conditional dissipation is explained, as well as the link between a multimode spectrum and the nonlinearity of the conditional diffusion.

[1] B. Castaing, G. Gunaratne, F. Heslot, L. Kadanoff, A. Libchaber, S. Thomae, X. Wu, S. Zaleski, and G. Zanetti, "Scaling of hard thermal turbulence in Rayleigh-Bénard convection," J. Fluid Mech. **204**, 1 (1989).
[2] F. Heslot, B. Castaing, and A. Libchaber, "Transition to turbulence in helium gas," Phys. Rev. A **36**, 5870 (1987).
[3] J. P. Gollub, J. Clarke, M. Gharib, B. Lane, and O. N. Mesquita, "Fluctuations and transport in a stirred fluid with a mean gradient," Phys. Rev. Lett. **67**, 3507 (1991).
[4] B. R. Lane, O. N. Mesquita, S. R. Meyers, and J. P. Gollub, "Probability distributions and thermal transport in a turbulent grid flow," Phys. Fluids A **5**, 2255 (1993).
[5] Jayesh and Z. Warhaft, "Probability distribution, conditional dissipation, and transport of passive temperature fluctuations in grid-generated turbulence," Phys. Fluids A **4**, 2292 (1992).
[6] M. R. Overholt and S. B. Pope, "Direct numerical simulation of a passive scalar with imposed mean gradient in isotropic turbulence," Phys. Fluids **8**, 11 (1996).
[7] E. S. C. Ching and Y. K. Tsang, "Passive scalar conditional statistics in a model of random advection," Phys. Fluids **9**, 5 (1997).
[8] A. Pumir, B. Shraiman, and E. D. Siggia, "Exponential tails and random advection," Phys. Rev. Lett. **66**, 2984 (1991).
[9] E. S. C. Ching and Y. Tu, "Passive scalar fluctuations with and without a mean gradient: A numerical study," Phys. Rev. E **49**, 1278 (1994).
[10] K. Ngan and R. T. Pierrehumbert, "Spatially correlated and inhomogeneous random advection," Phys. Fluids **12**, 822 (2000).
[11] R. T. Pierrehumbert, "Lattice models of advection-diffusion," Chaos **10**, 61 (2000).
[12] Y. Hu and R. T. Pierrehumbert, "The advection-diffusion problem for stratospheric flow. Part I: Concentration probability distribution function," J. Atmos. Sci. **58**, 1493 (2001).
[13] A. J. Majda and P. R. Kramer, "Simplified models for turbulent diffusion: theory, numerical modelling, and physical phenomena," Phys. Rep. **314**, 237 (1999).
[14] A. J. Majda, "The random uniform shear layer: an explicit example of turbulent diffusion with broad tail probability distributions," Phys. Fluids A **5**, 1963 (1993).
[15] R. M. McLaughlin and A. J. Majda, "An explicit example with non-Gaussian probability distribution for nontrivial scalar mean and fluctuation," Phys. Fluids **8**, 536 (1996).
[16] J. C. Bronski and R. M. McLaughlin, "Rigorous estimates of the tails of the probability distribution function for the random linear shear model," J. Stat. Phys. **98**, 897 (2000).
[17] E. Vanden Eijnden, "Non-Gaussian invariant measures for the Majda model of decaying turbulent transport," Commun. Pure Appl. Math. **54**, 1146 (2001).
[18] A. Bourlioux and A. J. Majda, "Elementary models with PDF intermittency for passive scalars with a mean gradient," Phys. Fluids **14**, 881 (2002).
[19] S. B. Pope and E. S. C. Ching, "Stationary probability density functions: an exact result," Phys. Fluids A **5**, 7 (1993).
[20] E. S. C. Ching, "General formula for stationary or statistically homogeneous probability density functions," Phys. Rev. E **53**, 6 (1996).
[21] N. Peters, *Turbulent Combustion*, Cambridge Monographs on Mechanics (Cambridge University Press, Cambridge, 2000).
[22] A. M. Yaglom, *Correlation Theory of Stationary and Related Random Functions* (Springer-Verlag, Berlin, 1987), Vol. I.
[23] S. B. Pope, "The probability approach to the modelling of turbulent reacting flows," Combust. Flame **27**, 299 (1976).
[24] Ya. G. Sinai and V. Yakhot, "Limiting probability distributions of a passive scalar in a random velocity field," Phys. Rev. Lett. **63**, 1962 (1989).